AIP Journal of Applied Physics

Excitation of the l = 3 diocotron mode in a pure electron plasma by means of a rotating electric field

G. Bettega, B. Paroli, R. Pozzoli, and M. Romé

Citation: Journal of Applied Physics **105**, 053303 (2009); doi: 10.1063/1.3086619

View online: http://dx.doi.org/10.1063/1.3086619

View Table of Contents: http://scitation.aip.org/content/aip/journal/jap/105/5?ver=pdfcov

Published by the AIP Publishing

Excitation of the $l=3$ diocotron mode in a pure electron plasma by means of a rotating electric field

G. Bettega, B. Paroli, R. Pozzoli, and M. Romé[a)]
Dipartimento di Fisica and I.N.F.N. Sezione di Milano, Università degli Studi di Milano, Via Celoria 16, I-20133 Milano, Italy

(Received 5 August 2008; accepted 16 January 2009; published online 3 March 2009)

The $l=3$ diocotron mode in an electron plasma confined in a Malmberg–Penning trap has been resonantly excited by means of a rotating electric field applied on an azimuthally four-sectored electrode. The experimental observations are interpreted with a theory based on the linearization of the drift-Poisson equations and by means of two-dimensional particle-in-cell simulations. The experimental technique presented in this paper is able to selectively excite different diocotron perturbations and can be efficiently used for electron or positron plasma control and manipulation.
 [DOI: 10.1063/1.3086619]

I. INTRODUCTION

An electron plasma can be confined for a very long time in a Malmberg–Penning cylindrical trap.[1] In a wide range of experimental parameters, the axially averaged electron plasma dynamics is analogous to that of a two-dimensional (2D) ideal fluid with uniform density. The flow vorticity ζ is proportional to the plasma density n, and the stream function ψ is proportional to the electrostatic potential ϕ.[2] The linear modes of the system are the diocotron modes (Kelvin modes in the ideal fluid case), i.e., potential and density perturbations with a spatial dependence of the form $\exp(il\theta)$, where the integer l is the azimuthal wave number. An electron plasma column with a monotonically decreasing radial density profile (or a stepwise density profile in the cold plasma limit) is stable against diocotron perturbations.[3] Under these conditions, the amplitude of a diocotron mode can be significantly increased when a suitable time- and space-dependent potential is applied to the boundary. To this aim, azimuthally sectored cylinders can be used as driving electrodes. For instance, the $l=1$ mode can easily be excited applying a nonzero potential on a single azimuthal sector; the $l=2$ mode (elliptical deformation of the plasma cross section) was excited by means of a voltage pulse[4] or more recently by means of a tuned resonant drive[5] using small amplitude time-dependent voltages on a four-sectored electrode, thus producing a nonrotating amplitude modulated quadrupole perturbation; and the $l=3$ mode was excited using a six-sectored electrode with static potential perturbations.[6]

Finding an experimental technique to selectively excite different diocotron perturbations is an important issue in the field of electron or positron plasma control and manipulation.[7] Therefore, simple driving systems suitable for the excitation of different diocotron modes are of particular interest. The goal of the paper is to show that a simple four-sectored electrode can be conveniently used to resonantly produce neat $l=3$ perturbations of the plasma column (triangular deformations of the plasma cross section), while the ubiquitous $l=1$ mode is maintained to a controllable amplitude.

The experimental technique and the basic theoretical model are described in Sec. II. The experimental results and their comparison with numerical simulations are presented in Sec. III. Short conclusions are drawn in Sec. IV.

II. EXPERIMENTAL APPARATUS AND TECHNIQUE

The experiments have been performed in the Malmberg–Penning trap ELTRAP.[8] A low density ($n \approx 10^{12}-10^{13}$ m^{-3}) and low temperature ($T \approx 1-10$ eV) electron plasma is contained within a stack of ten cylindrical electrodes (length $L=9$ cm, inner radius $R_W=4.5$ cm), kept under ultrahigh vacuum conditions ($p \approx 10^{-9}$ mbar). A schematic of the trap is shown in Fig. 1 (only six electrodes are drawn for convenience). The electron plasma is generated by a thermionic cathode and is axially confined by two negative potentials applied to the C3 and C6 electrodes, while the inner electrodes are usually grounded. The total plasma length is $L_P \approx 50$ cm. The S2 and S4 cylinders (length $L_S=15$ cm) are sectored with two and four sectors, respectively. The radial confinement is provided by a constant and uniform axial magnetic field $\mathbf{B}=B\mathbf{e}_z$ (up to 0.2 T, with $\mathbf{e}_z$ the unit vector along the trap axial direction), which keeps the plasma in azimuthal rotation. For an ideal flat density profile the equilibrium rotation frequency is $\omega_D=en/2\epsilon_0 B=\omega_p^2/2\omega_c$, where $-e$ is the electron charge and ϵ_0 is the vacuum permittivity.

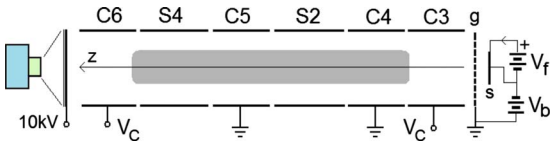

FIG. 1. (Color online) Schematic of the Malmberg–Penning trap ELTRAP. The plasma is axially trapped between C3 and C6 cylinders, biased at $|V_C| \leq 100$ V. The electrons are generated by a thermionic cathode (S) powered with a constant voltage (V_f) and negatively biased (V_b) with respect to a grounded grid (g). The imaging system consists of a phosphor screen and a CCD camera (on the left). The externally applied magnetic field is directed along the axis of the trap (z-axis).

[a)]Electronic mail: rome@mi.infn.it.

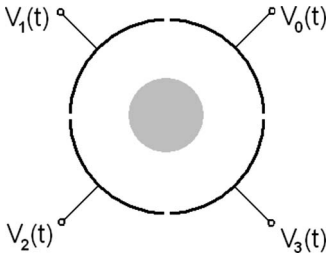

FIG. 2. Experimental configuration of the rotating wall experiment. Four $\pi/2$-phase-shifted signals are applied to the sketched electrodes in order to obtain an azimuthally rotating electrostatic perturbation.

The quantity ω_D is known as diocotron frequency and sets the characteristic time scale of the $\mathbf{E}\times\mathbf{B}$ collective plasma modes. After a given trapping time, the plasma is dumped against a positively biased phosphor screen grounding the electrode C6. The light emitted by the phosphor screen is collected by a charge coupled device (CCD) camera obtaining a snapshot of the axially averaged plasma density distribution.

$\pi/2$-phase-shifted sinusoidally time-varying potentials are applied to the four azimuthal sectors of the S4 electrode in order to excite the diocotron modes (see Fig. 2). The boundary potential reads

$$\delta\phi(r=R_W,\theta,t)=\sum_{m=0}^{3}V_m(t)[H(\theta-m\pi/2)-H(\theta-(m+1)\pi/2)], \quad (1)$$

where $V_m=V_d\cos(\omega_d t+\sigma m\pi/2)$ with $\sigma=\pm 1$, and V_d and ω_d are the amplitude and frequency of the external drive, respectively. The symbol H denotes the Heaviside step function.

The expression (1) can be written as a superposition of azimuthally propagating waves as

$$\delta\phi(r=R_W,\theta,t)=\frac{2\sqrt{2}}{\pi}V_d\sum_{n=1}^{\infty}\left\{\frac{1}{4n-3}\cos\left[\omega_d t+\sigma(4n-3)\theta-\sigma\frac{\pi}{4}\right]-\frac{1}{4n-1}\cos\left[\omega_d t-\sigma(4n-1)\theta-\sigma\frac{\pi}{4}\right]\right\}. \quad (2)$$

Referring to the rotation of the $n=1$ component in this expression, the cases $\sigma=-1$ and $\sigma=+1$ are denoted as "co-" and "counter-rotating" drives with respect to the plasma motion, respectively (the vorticity of the electron fluid is positive). Note that with the adopted phase relationship between the potentials on the four azimuthal sectors, only odd modes appear in Eq. (2) with alternating signs. This fact suggests how to excite higher order odd modes avoiding the excitation of the lowest $l=1$ diocotron mode.

This result is easily obtained within the framework of a linear treatment. Using a stepwise unperturbed radial density profile $n_0(r)=n_0H(R_P-r)$, where R_P is the radius of the plasma, a perturbation $\delta\phi=\epsilon\exp(il\theta-i\omega_d t)$ of the boundary potential produces a potential perturbation on the plasma surface of the form

$$\delta\phi(r=R_P,\theta,t)=\epsilon\left(\frac{R_P}{R_W}\right)^l\left[\frac{l\omega_D-\Omega_l}{\omega_d-\Omega_l}\exp(il\theta-i\Omega_l t)+\frac{l\omega_D-\omega_d}{\Omega_l-\omega_d}\exp(il\theta-i\omega_d t)\right], \quad (3)$$

where $\Omega_l\equiv\omega_D[l-1+(R_P/R_W)^{2l}]$ is the frequency of the lth diocotron mode. Here, $l>0$ and the potential on the boundary co-rotates with the plasma (all modes propagate in the positive θ-direction when the magnetic field is in the positive z-direction). Significant deformations of the plasma surface can occur only when $\omega_d=\Omega_l$. In this case

$$\delta\phi(r=R_P,\theta,t)=\epsilon\left(\frac{R_P}{R_W}\right)^l[1+i(l\omega_D-\Omega_l)t]\times\exp(il\theta-i\Omega_l t), \quad (4)$$

and the amplitude of the potential perturbation grows linearly with time. Therefore, for a co-rotating drive the diocotron modes $l=1,5,9,\ldots$ can be resonantly excited on a four-sectored electrode, while a counter-rotating drive induces a resonant excitation of the modes $l=3,7,11,\ldots$. In the following, the attention is focused on the results obtained for the $l=3$ mode. Note that when this mode is excited, the $l=1$ mode is not resonant and maintains a constant amplitude.

The previous computation of the linear response of the plasma to the external drive can be obviously generalized to the case of an arbitrary number of sectors.

III. EXPERIMENTAL ANALYSIS OF THE EXCITATION OF THE *L*=3 MODE

In the experiments the counter-rotating field has been applied for a fixed time interval Δt after an initial period of 0.5 s of free plasma evolution necessary to reach a thermal equilibrium state, which is characterized by an almost flat radial density profile. The error introduced by the phase shifter on the output signals due to the electronics transients imposes the use of a relatively long drive time $\Delta t=100$ ms. The plasma is dumped against the phosphor screen just after the drive is switched off.

The magnetic field strength has been fixed while the frequency of the drive has been varied searching for resonances. The observed behavior of the plasma density distribution versus the frequency of the applied counter-rotating drive is shown in Fig. 3. In the linear regime it is difficult to evaluate the effect of the perturbation potential directly from the CCD images, although close to the resonance frequency the maximum deformation of the plasma cross section is detected (lower left panel in Fig. 3). When the potential perturbation is continuously applied under resonance conditions, nonlinear effects may also be observed like the formation of ghost vortices[9] due to radial particle transport, as shown in Fig. 4.

The deformation of the plasma cross section has been chosen as a measure of the mode excitation level. This parameter has been evaluated calculating the position of the center of charge (after subtracting a background image obtained without trapped particles) and then finding the contour of the plasma as a sampled function $R(\theta)$ in the reference

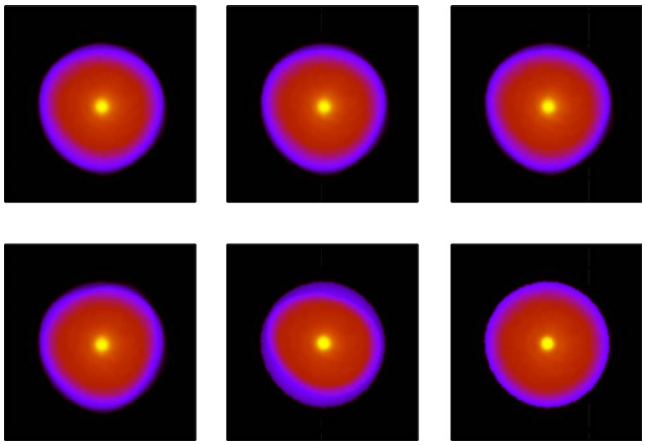

FIG. 3. (Color online) Plasma density distribution for different drive frequencies. From left to right, top to bottom: $\omega_d/2\pi=190$, 210, 215, 225, 245, and 250 kHz. The magnetic field strength is $B=0.117$ T and the drive amplitude is $V_d=2.2$ V.

frame of the center of charge. The Fourier transform of $R(\theta)$ finally isolates the contribution of interest $A^{(l)}$ of the boundary deformation. This method works fine as long as filaments and holes of the plasma density do not appear.

The final deformation of the plasma cross section, which is observed on the phosphor screen, is very sensitive to the number of applied drive periods due to the beating between the drive and the diocotron mode. In general, several beating periods occur during the application of the external field. For this reason, the values of the $A^{(3)}$ Fourier coefficients have been obtained repeating the experiment several times (typically 30 times) at fixed drive frequency and selecting the case corresponding to the maximum deformation. The behavior of $A^{(3)}$ versus the drive frequency is shown in Fig. 5 (left). The resonance curves appear quite broad due to the above mentioned effects. On the same figure (on the right), data relevant to the case of excitation with the opposite rotation are shown. As expected, the $l=3$ mode amplitudes are very small in comparison with the previous case. A similar but opposite behavior is detected, at lower frequencies, for the fundamental $l=1$ diocotron mode (not reported here).

The experimental observations have been validated by means of numerical simulations, analyzing both the co- and the counter-rotating external field cases using an external drive frequency $\omega_d \simeq \omega^{(1)}$ and $\omega_d \simeq \omega^{(3)}$. A 2D particle-in-cell (PIC) code moving N macroparticles on a Cartesian mesh

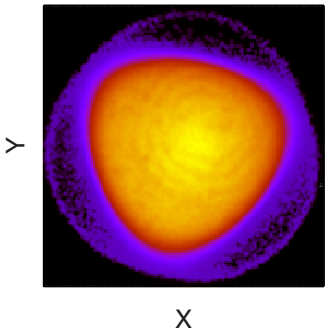

FIG. 4. (Color online) Formation of nonlinear structures close to the resonance condition ($B=0.067$ T and $\omega_d/2\pi=320$ kHz.)

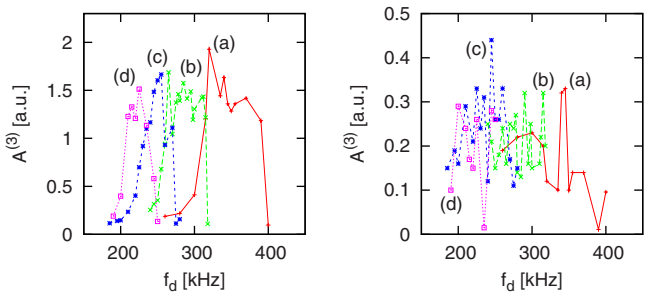

FIG. 5. (Color online) $A^{(3)}$ Fourier coefficient of the plasma contour vs the R_W drive frequency. Left: counter-rotating drive; right: co-rotating drive. The data refer to (a) $B=0.067$ T, (b) $B=0.1$ T, (c) $B=0.117$ T and (d) $B=0.133$ T. The drive amplitude is $V_d=2.2$ V.

has been used. The code solves the drift-Poisson equations written in terms of the normalized quantities $\tilde{r}=r/R_W$, $\tilde{n}=n/n_0$, $\tilde{\phi}=\phi(\epsilon_0/en_0R_W^2)$, $\tilde{v}=v(\epsilon_0 B/en_0R_W)$, and $\tilde{t}=t(en_0/\epsilon_0 B)$. With this normalization a period of the azimuthal equilibrium rotation of the plasma column corresponds to $\tau_{\rm rot}=4\pi$, and the normalized equilibrium rotation frequency is $\tilde{\omega}_D=1/2$. The particle positions are advanced using a fourth-order Runge–Kutta scheme, while the electrostatic potential is calculated at each time step with a standard relaxation routine. Time varying boundary conditions are used, which reproduce the rotating wall experiments. The numerical simulations are performed using typically a 256×256 mesh, $N=10^5$ macroparticles, and a time step $dt=\tau_{\rm rot}/1000$. An initial condition of uniform density with radius $R_P/R_W=0.3$ is considered, corresponding to the measured mean plasma radius.

If the drive is counter-rotating and $\omega_d \simeq \omega^{(3)}$, the destabilization of the $l=3$ mode predicted by the linear model occurs. Setting ω_d to the theoretical value of the resonance

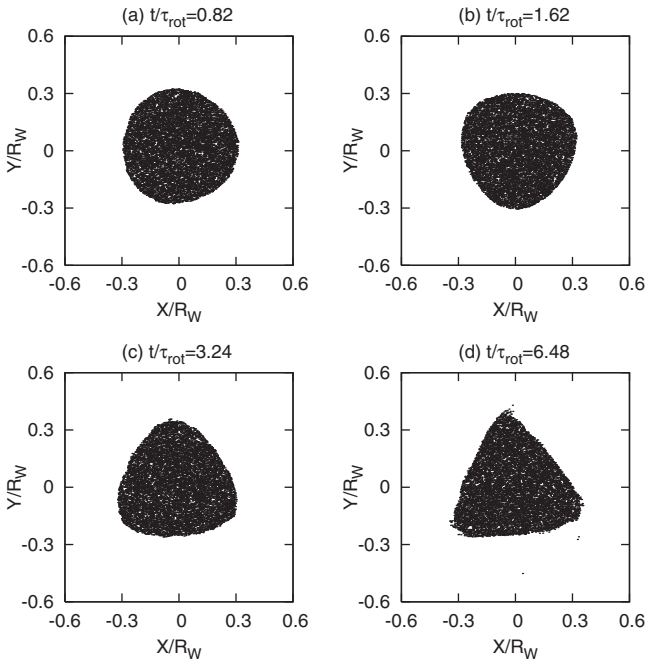

FIG. 6. Particle distributions obtained with a PIC simulation of the interaction of a counter-rotating drive with $\tilde{V}_d=10^{-2}$ and $\omega_d \simeq \omega^{(3)}$. The times are indicated directly on the plots.

frequency, the simulation shows an evolution toward a well defined triangular plasma cross section (see Fig. 6), which becomes evident after a few characteristic times τ_{rot}.

IV. CONCLUSIONS

The effectiveness of a method to excite the $l=3$ diocotron mode in a pure electron plasma has been investigated in the ELTRAP device. The technique relies on the application of phase-shifted time-dependent potentials on a four-sectored electrode. The $l=1$ component of the applied field rotates in the opposite direction with respect to the $l=3$ mode propagation. The experimental results have been interpreted theoretically with a linearized 2D drift-Poisson model and compared with 2D PIC simulations. Both in the experiments and in the simulations, close to resonance conditions the $l=3$ perturbation grows initially linearly with time, determining a triangular deformation of the plasma cross section.

The experimental technique presented here can be efficiently used for plasma manipulation. In the case of an arbitrary even-sectored electrode it allows to excite higher order odd diocotron modes with a counter-rotating electric field.

[1]J. H. Malmberg and J. S. deGrassie, Phys. Rev. Lett. **35**, 577 (1975).
[2]C. F. Driscoll and K. S. Fine, Phys. Fluids B **2**, 1359 (1990).
[3]R. C. Davidson, *An Introduction to the Physics of Nonneutral Plasmas* (Addison-Wesley, Redwood City, 1990).
[4]A. C. Cass, Ph. D. dissertation, University of California at San Diego (1998).
[5]G. Bettega, F. Cavaliere, B. Paroli, M. Cavenago, R. Pozzoli, and M. Romé, Phys. Plasmas **14**, 102103 (2007).
[6]R. Chu, J. S. Wurtele, J. Notte, A. J. Peurrung, and J. Fajans, Phys. Fluids B **5**, 2378 (1993).
[7]J. R. Danielson, T. R. Weber, and C. M. Surko, Phys. Plasmas **13**, 123502 (2006).
[8]M. Amoretti, G. Bettega, F. Cavaliere, M. Cavenago, F. De Luca, R. Pozzoli, and M. Romé, Rev. Sci. Instrum. **74**, 3991 (2003).
[9]X. P. Huang, K. S. Fine, and C. F. Driscoll, Phys. Rev. Lett. **74**, 4424 (1995).